Proceedings of the ASME 2015 International Mechanical Engineering Congress and Exposition
IMECE2015
November 13-19, 2015, Houston, Texas

IMECE2015-52997

PARAMETRIC STUDY ON THE EFFECT OF PARTIAL CHARGE ON WATER INFILTRATION BEHAVIOR IN MFI ZEOLITES

Geoffrey A. Vaartstra[1], Tom Humplik[2], Evelyn N. Wang[2], Shalabh C. Maroo[1*]
[1]Department of Mechanical and Aerospace Engineering, Syracuse University, Syracuse, NY, USA
[2]Department of Mechanical Engineering, Massachusetts Institute of Technology, Cambridge MA, USA
[*]Email: scmaroo@syr.edu

ABSTRACT

This work analyzes the infiltration behavior of water into sub-nanometer MFI zeolite pores using molecular dynamics simulations. Infiltration simulations are run for a range of partial charge values on the zeolite atoms. Infiltration behavior is compared to partial charges to verify dependence and determine critical charge above which infiltration becomes severely inhibited even at high pressures. Attraction energy is calculated and correlated to the observed infiltration behavior. The critical partial charge of Si~1.8 occurs when the water-zeolite interaction energy becomes stronger than water-water attraction due to which water molecules get stuck and infiltration is significantly reduced.

INTRODUCTION

MFI zeolites are crystalline aluminosilicates with uniform sub-nanometer pores having tetrahedrally bonded silicon (Si), aluminum (Al) and oxygen (O) atoms in their nanoporous framework structures. The zeolite framework is composed of elliptical straight pores (0.53 nm × 0.56 nm), elliptical zig-zag (sinusoidal) pores (0.55 nm × 0.51 nm) and intersections. The approximate diameter of a water molecule is 0.28 nm. Thus, the pore size restricts water into a single molecular chain presenting an extraordinary physical behavior of extreme confinement. Zeolites have been shown to achieve water filtration or desalination [1-5] based on the principle of size exclusion, i.e. water molecules can pass through while the larger solvated ions (~0.7-0.8 nm) cannot.

The sub-nanometer pore size limits the experimental techniques which can be applied to zeolites. Raman scattering, nuclear magnetic resonance, X-ray diffraction, neutron scattering, neutron diffraction, and pressurized water infiltration have provided some implicit information on the structural, dynamic and thermodynamic behavior of water [6-8]; however, complete physical understanding to predict the dynamical properties and transport of water in zeolite pores is still lacking from experimental measurements [9]. Hence, researchers have been utilizing molecular dynamics (MD) simulations to gain additional insights into the molecular interactions on how they govern the confinement behavior of water [9-14]. In these simulations, the force-field parameters define the force interactions between different atoms (e.g. Si, O, O_{water}, H_{water}, etc.) present in the system, and are the key towards obtaining realistic and physical behavior of nanoconfined water in the pores. Conflicting studies and inconsistencies, primarily due to the various force-fields adopted, have led to discrepancies [6, 8-10, 15].

A computational model which can capture the physical nature of water infiltration in MFI zeolites is crucial for the analysis of transport behavior. In order to assess the accuracy of the properties and parameters used in a given model, simulation results can be compared against properties which have been measured in laboratory experiments. Two quantities of interest when studying the infiltration behavior of water into sub-nanometer zeolite pores are infiltration pressure and framework capacity (internal water capacity) [8, 9]. Maroo et al. observed maximum infiltration at ~100 MPa and a capacity of ~48 water molecules per unit cell in infiltration experiments, yet noted a discrepancy between the observed capacity and simulation results [9]. A key parameter affecting simulated results is the partial charge assigned to the Si and O atoms of the zeolite crystal. Researchers have used a variety of partial charges to model MFI and other zeolite types for many applications [10, 11, 13, 14, 16, 17]. Adjusting partial charge while holding other simulation parameters constant has been seen to change the infiltration behavior of water [9] due to the attraction energy the water molecules experience to both the zeolite and other water

molecules. MFI type zeolites have a well-defined structure [18], thus there is no need to consider changes in pore geometry due to partial charge. In this work, we conduct a parametric study to understand the dependence of attraction energies on assigned partial charge along with the subsequent infiltration behavior of water and study the elementary physics governing these nanoscale interactions.

METHODS

To simulate infiltration, an MFI zeolite crystal was constructed from a coordinate file produced by the database of zeolite structures [18] with dimensions 4.01800 nm × 3.9426 nm × 23.686 nm corresponding to the known measurements of MFI unit cells (u.c.) to form a crystal of 2 u.c. × 3 u.c. × 12 u.c. with the straight pores aligned parallel to the z-axis of the simulation box. An equilibrated water box with a pressure of 498.06 MPa was split and shifted along the z-axis to either side of the zeolite crystal, as seen in Fig. 1. Graphene walls, used for impermeability to water, were placed to enclose the outer boundaries of the bulk water. The simulation box was constructed with the same cross sectional area as the zeolite crystal and bulk water volumes and z-length of 95.286 nm, leaving 50 nm of vacuum space to prevent interaction between the volumes of water on either side of the zeolite. Water was modeled with SPC/E (defines charge, bond parameters, etc.) [19] and maintained at 298 K with the Berendsen thermostat. Simulations were run for 3000 ps at steps of 2 fs with interactions between the zeolite and water molecules modeled by the GROMOS force field. The Shift model with a cut-off radius of 1 nm was used to calculate both Electrostatic and Van der Waals interactions. To investigate the effect of partial charge on the infiltration behavior of the water molecules, the same simulation was replicated with all parameters held constant aside from varying partial charges assigned to the Si and O atoms of the zeolite crystal. This was done is such a way that the charges on Si ranged from 0 to 3, as to include values used in prior literature [10, 11, 13, 14, 16, 17], and corresponding charges O=-Si/2.

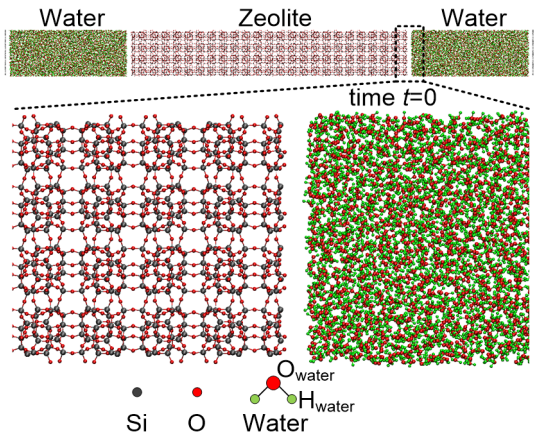

Figure 1: Initial domain with zeolite crystal surrounded by water molecules bounded by graphene walls.

Attraction energy of water molecules in unit cell 1 (u.c.1) to the zeolite and to the bulk water was analyzed using PME to calculate coulomb interactions for a single-step simulation with all atoms frozen from the output of the infiltration simulation. This required separate energy simulations for each group, as seen in Tables 1 and 2, in order to accurately solve for the reciprocal (long range) coulomb energy between the respective groups. These isolated reciprocal space interactions were then combined with real space interactions, both coulomb from PME and Lennard-Jones as calculated by Shift, and averaged per water molecule. This calculation was repeated for trajectory frames at intervals of 10 ps for the entire 3000 ps span of infiltration, with average energy of interaction values for the given partial charge being considered from the final 500 ps, when energies were stable.

Table 1: Steps involved in calculating the water-to-zeolite interaction energy

water-zeolite	
+	Reciprocal of system of water in u.c. 1 and zeolite
-	Reciprocal of isolated zeolite
-	Reciprocal of isolated u.c. 1 water molecules
=	water-zeolite reciprocal contribution

Table 2: Steps involved in calculating the water-to-water interaction energy

water-water	
+	Reciprocal of all water molecules
-	Reciprocal of system excluding u.c. 1 water molecules
=	water-water reciprocal contribution

In order to measure the pressure of bulk water in water-zeolite molecular dynamics simulations using GROMACS [20], a curve-fitted equation was created to relate the pressure as recorded by the software to the density of water molecules, which can be easily calculated from trajectory files. Separate simulations were run for water in simulation boxes constructed with fixed volume at varying densities. Using the SPC/E model for water, the water simulations were equilibrated for 1000 ps in steps of 2 fs at a temperature of 298 K maintained by the Berendsen thermostat. Electrostatic interactions were calculated using the PME model with a cut-off radius of 1.3 nm while Van der Waals force interactions were calculated using the Shift model with a cut-off radius of 1 nm. Each simulation box had dimensions 4.01800 nm × 3.9426 nm × 20 nm with periodic boundaries and the GROMOS force field was used. The final recorded pressures were the average values for the last 300 ps of the corresponding equilibrium simulation as reported by GROMACS.

RESULTS AND DISCUSSION

The relation between pressure and density of bulk water as observed by GROMACS was shown to fit well with NIST data [21] documenting the accepted densities at given pressures

(Figure 2). This validates the ability to compare infiltration pressures from molecular dynamics simulations with experimental data [6, 8, 9, 15] while yielding a curve-fitted equation (Equation 1) with which to calculate bulk pressure from density during simulation:

$$P = 0.0086\rho^2 - 15.372\rho + 6818 \quad \ldots(1)$$

where P is the bulk pressure of water and ρ is the density. For the purpose of this work, the pressure calculation has been used as a measure of infiltration where final pressure and infiltration are inversely related, i.e. lowering of bulk pressure is a result of water entering the zeolite pores.

In agreement with prior literature [9], water infiltration simulations showed a clear dependence of infiltration on partial charge. From low values starting at Si=0, infiltration is high and increases with charge value. Seen in Figure 3, a maximum rate occurs near Si=1.2, showing optimal conditions for water to enter the crystal pores before attraction to the zeolite atoms becomes too strong. Then small increases in charge for values near Si=1.6-1.8 and above cause large decreases in infiltration until the rate approaches a steady minimum at Si=2.4 and higher. This trend is inferred from the final equilibrated bulk water pressure vs. charge plot (Figure 3) that pressure drop in bulk liquid is a result of water infiltrating the zeolite.

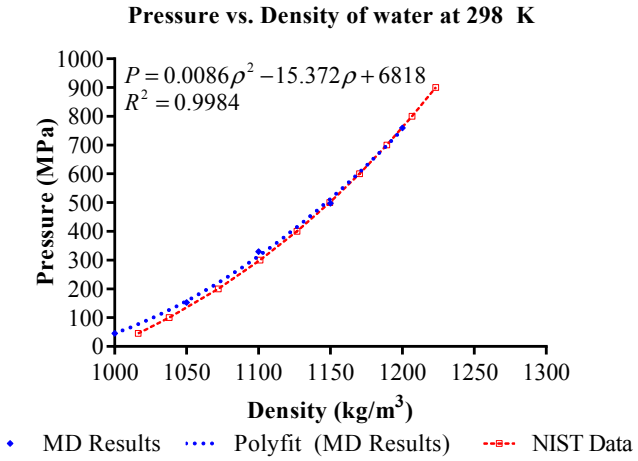

Figure 2: Density vs. Pressure of water at 298 K. The two sets of data compare well and a curve-fitted equation was derived from the MD Results to calculate pressure in simulations.

By analyzing the attraction energy to both water and zeolite experienced by water molecules contained in the u.c.1 layer, it is seen in Figure 6 that the water-water attraction is significantly higher than water-zeolite attraction for low charge values (~1) and molecules are able to enter the pores. Once charge values are sufficiently high (~2), water-water attraction is seen to be much lower than water-zeolite attraction. Under these conditions, a small number of water molecules enter the pores and get 'stuck' as a result of the comparatively stronger attraction to the zeolite, restricting additional molecules from infiltrating. For example, at Si=2.8 (Figure 5) water-zeolite attraction is higher than water-water attraction and many fewer water molecules are seen to infiltrate u.c.1 compared to Si=0.2 (Figure 4) where the higher attraction is water-water. These results (Figures 3, 4, 5) also suggest that framework capacity depends on partial charge. This is a relation of particular interest to further investigate since framework capacity can be directly compared against experimental results. In this work, the results show that the unit cell capacity at the recorded pressures is greater than 40 water molecules per u.c. for all partial charges less than or equal to Si=2.0, higher than the experimental capacity of 35.5 ± 1.8. For all charge values above Si=2.0, peak capacity was not reached under the time and pressure parameters of the simulation. Ongoing research will further investigate capacities for these simulations, along with altering the partial charges on the water molecule.

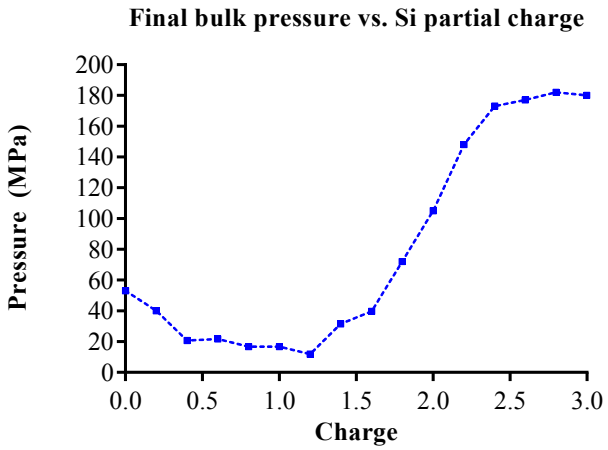

Figure 3: Final bulk pressure after 3000 ps vs. partial charge on Si, all initial pressures were 498.06 MPa.

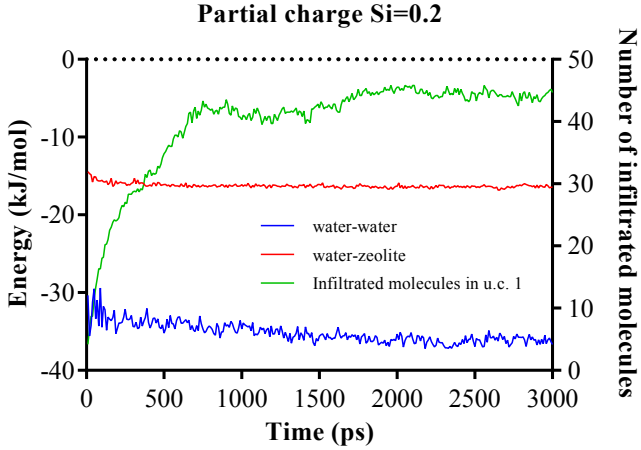

Figure 4: Attraction energy of infiltrated water in u.c.1 to water and zeolite for a low partial charge value. With a much greater attraction to water, molecules infiltrate easily and fill u.c.1 to capacity.

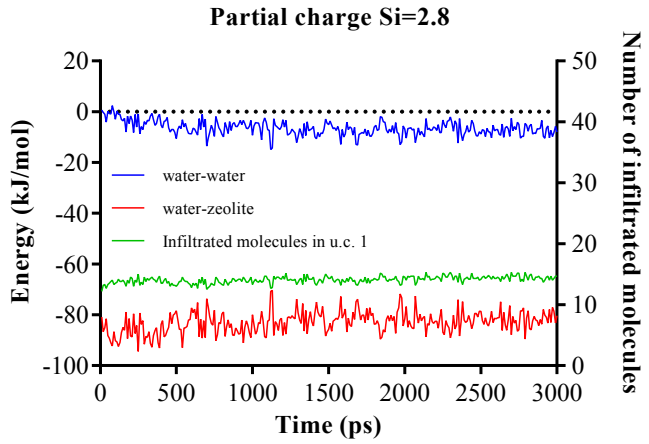

Figure 5: Attraction energy of infiltrated water in u.c.1 to water and zeolite for a high partial charge value. As the attraction to the zeolite is now greater, molecules are unable to freely infiltrate the zeolite pores.

The resulting trends of attraction energies for varying charges as seen in Figure 6 fit well with the observed infiltration tendencies. As expected, water enters the zeolite pores for all charge values where water-water attraction is greater than water-zeolite attraction. The steep decline of infiltration rate near Si=1.6-1.8 reflects conditions where entrance is slowed as molecules have a similar attraction to both water and zeolite. Because the water-zeolite attraction increases so quickly in proportion to changes in charge after the equilibrium point, it makes sense that infiltration approaches a minimum rapidly as charge values increase past Si=1.8. Comparing attraction energy to infiltration data, it is expected that higher infiltration pressures will be required to overcome stronger interactions with the zeolite for charges past the equilibrium point.

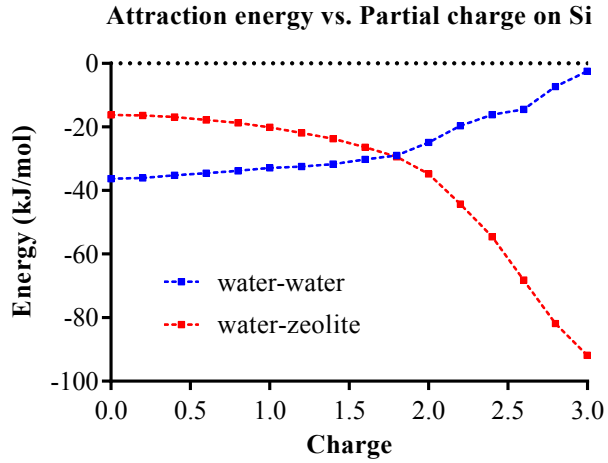

Figure 6: Attraction energy taken as an average from the final 500 ps vs. partial charge on Si. Attraction to water is greater for low charge values until the energies reach equality near Si=1.8, after which attraction to zeolite quickly becomes much stronger.

CONCLUSION

A density vs. pressure curve was established for water in MD simulations. By close fit to accepted NIST values, this curve validates the comparison of infiltration versus pressure curves obtained from simulations to those from laboratory experiments. A curve-fitted equation was extracted and used to measure the pressure of bulk water during infiltration simulations. Holding all other parameters constant, infiltration was simulated for partial charge on Si ranging from 0 to 3.0 in steps of 0.2 for 3000 ps. Using final pressure as a measurement of infiltration, it was determined that maximum infiltration occurs near Si=1.2 and that infiltration rate rapidly declines as charge increases past Si=1.6. Attraction energy calculations showed that infiltration depends on the influence of both water-water attraction and water-zeolite attraction, where a significantly stronger water-zeolite attraction inhibits infiltration. Average attraction energies for the final 500 ps of each simulation were plotted against the corresponding charge value to map tendencies of attraction as assigned partial charge is varied, which were shown to correlate as expected to infiltration behavior. Additionally, a dependence of framework capacity on partial charge assignment was observed, which can be further investigated to find partial charge values yielding simulation results that compare well with experimental observations. In addition to the data presented in this work, continued research is in progress to address the correlation between partial charge assignment and required infiltration pressure.

REFERENCES

1. Drobek, M., et al., *Long term pervaporation desalination of tubular MFI zeolite membranes.* Journal of Membrane Science, 2012. **415**: p. 816-823.
2. Humplik, T., T. Laoui, and E.N. Wang, *Transport across Sub-Nanometer Zeolite Pores for Water Desalination.* Proceedings of the 8th International Conference on Nanochannels, Microchannels and Minichannels, 2010, Pts a and B, 2011: p. 1383-1387.
3. Humplik, T., et al., *Nanostructured materials for water desalination.* Nanotechnology, 2011. **22**(29).
4. Liu, Y. and X. Chen, *High permeability and salt rejection reverse osmosis by a zeolite nano-membrane.* Phys Chem Chem Phys, 2013. **15**(18): p. 6817-24.
5. Li, L., J. Dong, and R. Lee, *Preparation of alpha-alumina-supported mesoporous bentonite membranes for reverse osmosis desalination of aqueous solutions.* J Colloid Interface Sci, 2004. **273**(2): p. 540-6.
6. Cailliez, F., et al., *Thermodynamics of water intrusion in nanoporous hydrophobic solids.* Physical Chemistry Chemical Physics, 2008. **10**(32): p. 4817-4826.
7. Humplik, T., et al., *Effect of Hydrophilic Defects on Water Transport in MFI Zeolites.* Langmuir, 2014. **30**(22): p. 6446-6453.

8. Humplik, T., et al., *Framework water capacity and infiltration pressure of MFI zeolites.* Microporous and Mesoporous Materials, 2014. **190**: p. 84-91.
9. Maroo, S.C., et al., *Water Infiltration in Zsm-5 Zeolites: Effect of Pore Volume and Water Structure.* Proceedings of the Asme Micro/Nanoscale Heat and Mass Transfer International Conference, 2012, 2012: p. 625-631.
10. Ahunbay, M.G., *Monte Carlo Simulation of Water Adsorption in Hydrophobic MFI Zeolites with Hydrophilic Sites (vol 27, pg 4986, 2011).* Langmuir, 2011. **27**(23): p. 14703-14703.
11. Ari, M.U., et al., *Molecular Dynamics Simulation of Water Diffusion in MFI-Type Zeolites.* Journal of Physical Chemistry B, 2009. **113**(23): p. 8073-8079.
12. Cailliez, F., et al., *Thermodynamic study of water confinement in hydrophobic zeolites by Monte Carlo simulations.* Molecular Simulation, 2009. **35**(1-2): p. 24-30.
13. Coasne, B., et al., *Molecular Simulation of Adsorption and Transport in Hierarchical Porous Materials.* Langmuir, 2013. **29**(25): p. 7864-7875.
14. Hughes, Z.E., et al., *A Computational Investigation into the Suitability of Purely Siliceous Zeolites as Reverse Osmosis Membranes.* Journal of Physical Chemistry C, 2011. **115**(10): p. 4063-4075.
15. Trzpit, M., et al., *The effect of local defects on water adsorption in silicalite-1 zeolite: a joint experimental and molecular simulation study.* Langmuir, 2007. **23**(20): p. 10131-9.
16. Bushuev, Y.G., et al., *Water-Hydrophobic Zeolite Systems.* Journal of Physical Chemistry C, 2012. **116**(47): p. 24916-24929.
17. Fischer, M. and R.G. Bell, *Modeling CO2 Adsorption in Zeolites Using DFT-Derived Charges: Comparing System-Specific and Generic Models.* Journal of Physical Chemistry C, 2013. **117**(46): p. 24446-24454.
18. Ch. Baerlocher, L.B.M., *Database of Zeolite Structures.*
19. Berendsen, H.J.C., J.R. Grigera, and T.P. Straatsma, *THE MISSING TERM IN EFFECTIVE PAIR POTENTIALS.* Journal of Physical Chemistry, 1987. **91**(24): p. 6269-6271.
20. Van der Spoel, D., et al., *GROMACS: Fast, flexible, and free.* Journal of Computational Chemistry, 2005. **26**(16): p. 1701-1718.
21. WebBook, N.C., *NIST Chemistry WebBook.*
22. Fischer, M. and R.G. Bell, *Influence of Zeolite Topology on CO2/N-2 Separation Behavior: Force-Field Simulations Using a DFT-Derived Charge Model.* Journal of Physical Chemistry C, 2012. **116**(50): p. 26449-26463.
23. Khosravi, A., et al., *The effects of partial charges and water models on water adsorption in nanostructured zeolites, application of PN-TrAz potential in parallel GCMC.* Molecular Simulation, 2013. **39**(6): p. 495-504.
24. Qiao, Y., L. Liu, and X. Chen, *Pressurized Liquid in Nanopores: A Modified Laplace-Young Equation.* Nano Letters, 2009. **9**(3): p. 984-988.
25. Zhu, B., et al., *Application of robust MFI-type zeolite membrane for desalination of saline wastewater.* Journal of Membrane Science, 2015. **475**: p. 167-174.